The field-orientation dependence of the 1D enhancement in Zeeman spin-splitting in InGaAs quantum point contacts

T. P. Martin,[1] A. Szorkovszky,[1] A. P. Micolich,[1] A. R. Hamilton,[1,*]
C. A. Marlow,[2] R. P. Taylor,[2] H. Linke,[2,3] and H.Q. Xu[3]

[1]*School of Physics, University of New South Wales, Sydney NSW 2052, Australia*
[2]*Department of Physics, University of Oregon, Eugene OR 97403, USA*
[3]*Division of Solid State Physics, Lund University, Box 118, S-221 00 Lund, Sweden*

(Dated: October 2, 2009)

We study the Zeeman spin-splitting in a quantum point contact (QPC) etched into an InGaAs/InP heterostructure for three orthogonal magnetic field orientations with respect to the QPC. For the two in-plane orientations we observe an isotropic Zeeman spin-splitting, which becomes stronger as the system is made more one-dimensional. The Lande g-factor is enhanced by up to a factor of two compared to two-dimensional electron systems in InGaAs/InP. A much larger Zeeman splitting is observed when the field is oriented perpendicular to the heterostructure, resulting in a g-factor of 15.7 in the one-dimensional limit.

PACS numbers: 73.21.Hb, 71.70.Ej, 85.75.-d

Quantum devices based on InGaAs/InP heterostructures hold considerable promise for spintronic applications due to their strong spin-orbit interaction and high transport mobility.[1] The strong spin-orbit interaction arises due to the narrow-band gap of InGaAs, which leads to a significantly higher Landé g-factor compared to more conventional materials, such as GaAs, that are commonly used for realizing quantum devices.[2–6] Additionally, it has recently been shown in both experimental[7–12] and theoretical[13–16] studies that further enhancement in the g-factor can be achieved by confining the carriers to a one-dimensional system such as a quantum wire or quantum point contact (QPC). This extra enhancement is due to the dominance of the exchange energy over the kinetic energy in low dimensions and at low electron densities.[13–15]

The 1D g-factor is not necessarily isotropic, depending both on the orientation of the field with respect to the 1D system, and in some cases, the orientation with respect to crystallographic axes. Despite some studies of the anisotropy of the Zeeman splitting in 1D hole systems in GaAs,[10,16,17], the directional dependence of the Zeeman splitting in 1D electron systems in InGaAs has not been fully explored. In this paper, we study the Zeeman splitting in an InGaAs/InP QPC device for three orthogonal orientations of the magnetic field with respect to the transport direction in the QPC. We find strong exchange enhancement for in-plane magnetic fields, and even stronger enhancement for perpendicular magnetic fields, with a peak g-factor of 15.7 achieved in this device.

The material used for this experiment was an $In_{0.75}Ga_{0.25}As$/InP heterostructure modulation doped with Si.[18,19] A 120 nm wide and 160 nm long QPC was defined with electron-beam lithography and shallow wet etching. The etch trenches are then back-filled with photoresist, and a Ti/Au top-gate is deposited to cover the entire structure. The 2D electron density and mobility, measured adjacent to the QPC on the same chip, are 6.6×10^{11} cm^{-2} and 200,000 cm^2/Vs at $T = 1.3$ K and zero gate bias.[19] Measurements were performed at a temperature of 1.3 K in three separate cool-downs with different magnetic field orientations: parallel to the heterostructure growth direction (B_z); in-plane and parallel to the QPC transport direction (B_x); and in-plane and perpendicular to the QPC transport direction (B_y). The QPC conductance G was measured in a four-probe configuration using lock-in amplification at 17 Hz with an a.c. excitation of 100 μV.

Figure 1(b) shows the classic staircase of quantized conductance plateaus as a function of the applied top gate bias V_g.[20] The evolution of the conductance and transconductance are shown for in-plane orientations B_x and B_y in the left (a-c) and right (d-f) panels of Fig. 1 respectively. To highlight the behavior of the 1D subbands we focus on the transconductance dg/dV_g, where $g = dI/dV$ is the differential conductance . High transconductance (light regions in the colormaps) correspond to the risers between the plateaus in the conductance g, where the Fermi energy E_F crosses the various 1D subband energies E_n.[7] In panels (a) and (d) the peaks in the transconductance (bright regions) split by a voltage δV_g as the magnetic field lifts the spin degeneracy of the 1D subbands. Similar splittings are observed in panels (c) and (f) when a d.c. source-drain bias V_{sd} is applied across the QPC at $B = 0$. For $V_{sd} \neq 0$ the chemical potentials in the source and drain reservoirs no longer coincide in energy, and the transconductance peaks separate by a gate voltage proportional to the bias energy eV_{sd}.[7]

We use a standard procedure that compares the splittings in B with those in V_{sd} to obtain the Zeeman energy splitting:[7,21,22]

$$\Delta E_Z = e\frac{dV_{sd}}{dV_g}\delta V_g(B) = |g_n^*|\mu_B B \qquad (1)$$

where $|g_n^*|$ is the effective g-factor of the n^{th} subband, $\delta V_g(B)$ is the splitting in gate voltage as a function

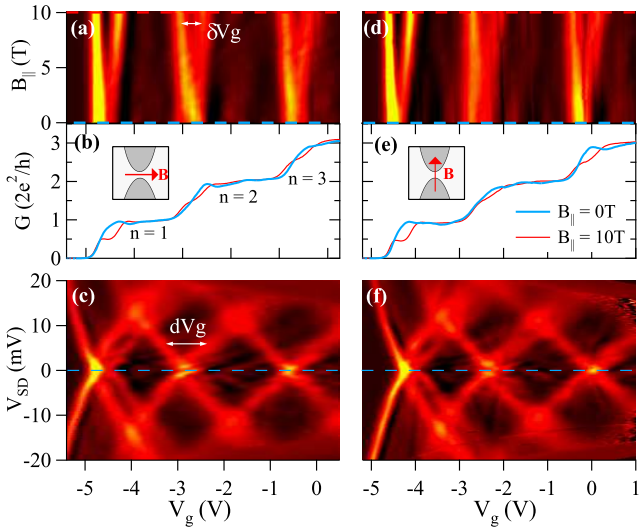

FIG. 1: (Color online) Zeeman spin-splitting induced by in-plane magnetic fields applied (left, B_x) perpendicular and (right, B_y) parallel to the QPC confinement. (a),(d): Transconductance dg/dV_g plotted versus gate voltage V_g and B, showing the evolution of each spin-degenerate transition into two spin-split transitions (light regions mark risers, i.e. the 1D subband transitions). (b),(e): Conductance g plotted versus V_g at $B = 0$ (blue) and 10 T (red). (c),(f): Transconductance dg/dV_g plotted versus V_g and d.c. source-drain bias V_{sd} at $B = 0$. The device was thermally cycled to 300 K between the measurements presented in panels (a–c) and those in (d–f). $T = 1.3$ K

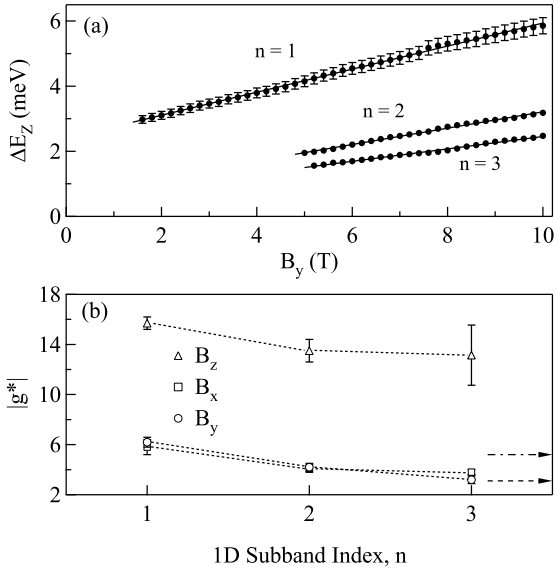

FIG. 2: (a) Zeeman splitting ΔE_Z plotted vs magnetic field B_y for the lowest three subbands. Solid lines show linear fits to the data. (b) Effective Landé g-factors $|g^*|$ measured in the QPC for the three magnetic field orientations B_x, B_y, and B_z. Dashed lines are guides to the eye. The upper and lower arrows on the right hand side indicate the bare 2D g-factors from Ref. 4 for B perpendicular and parallel to the quantum well respectively.

of B, and dV_{sd}/dV_g converts the splitting in gate voltage to an energy splitting. The Zeeman splittings for B_y obtained from the data in Figs. 1(d) and (f) are plotted in Fig. 2(a). The Zeeman splitting increases linearly with B_y and we calculate a field-independent $g_n^* = d(\Delta E_Z)/dB$ for each subband from the slope of the lines in Fig. 2(a). The finite intercept of the Zeeman splitting at $B = 0$ for the $n = 1$ subband is associated with the '0.7 anomaly' that has been extensively studied in GaAs systems.[7,8] Similar data is obtained for B_x,[11] with a linear Zeeman splitting again allowing a field independent g-factor to be extracted. Figure 2(b) shows $|g_n^*|$ for both in-plane orientations as a function of the subband index n. The g-factors for the two orientations agree within error (within 10% for $n = 3$), suggesting that the Zeeman splitting is isotropic for in-plane fields.

Measuring the Zeeman splitting when the magnetic field is perpendicular to the quantum well is more complex, since B_z couples to the orbital motion of the electrons and adds a harmonic potential to the QPC confinement.[5,19,23–25] At high magnetic fields, $B > 2\hbar k_F/eW_{qpc}$, the cyclotron diameter fits within the electrostatic width W_{qpc} of the QPC, and we enter the quantum Hall regime where the 1D subbands have evolved into 2D Landau levels.[25] To ensure that we are measuring the 1D g-factor, rather than simply measuring the 2D Landau level spacing, we restrict the measurement to fields $B_z \lesssim 5$ T where the electrostatic confinement dominates.

Fig. 3(a) shows the evolution of the 1D subbands in a perpendicular magnetic field, with dg/dV_g plotted as a function of V_g and B_z. The subband evolution shows a pronounced curvature due to the coupling of B_z to the orbital motion, in contrast to in-plane fields where the subbands split linearly (Figs. 1(a,d)). To ensure that our analysis is valid in this more complex regime we measure the Zeeman splitting using two independent techniques.

The first approach is to use the same method as for in-plane fields, measuring the Zeeman splitting ΔE_Z from the splittings of the transconductance peaks δV_g as a function of B_z. The δV_g are then converted to an energy by performing source-drain biasing. However, because B_z alters the confining potential in the QPC, it causes a curvature of the peak splittings and moves each peak to lower gate bias with increasing B_z. To account for this we performed source-drain biasing measurements at several different magnetic fields. An example is shown in Fig. 3(c) for $B_z = 4$ T. The conversion between gate voltage splitting and energy dV_{sd}/dV_g is plotted as a function of V_g for several different 1D subbands and magnetic fields in Fig. 3(c). Somewhat unexpectedly we find all the data fall onto a single trend-line independent of the magnetic field, which shows that the magnetic field does not affect the 'lever-arm' between the applied gate voltage and the 1D subband energies. We use the trend-line in

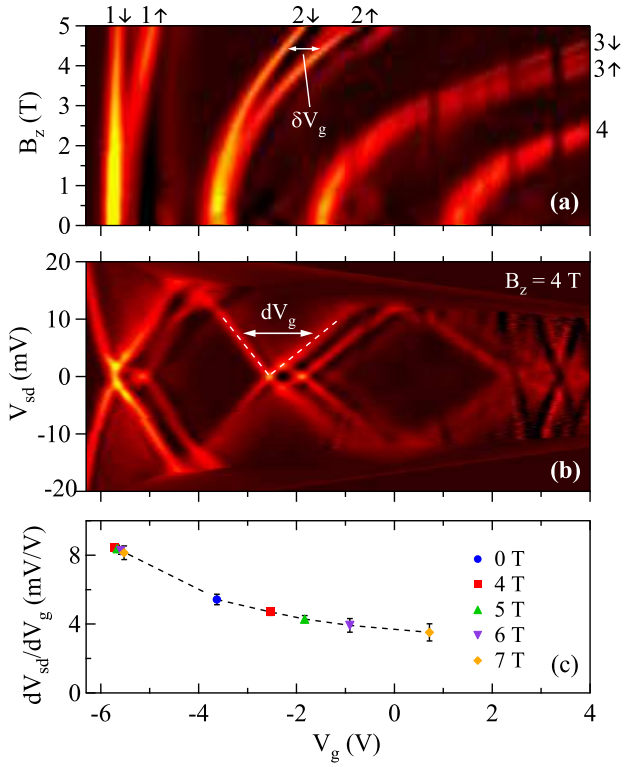

FIG. 3: (Color online) (a) Transconductance dg/dV_g plotted versus gate voltage V_g and magnetic field B_z applied perpendicular to the quantum well. Bright regions show the evolution of the subband edges with B_z. The labels $1\uparrow$ etc. indicate the subband index and the spin state of the various subbands. (b) Transconductance dg/dV_g plotted versus gate voltage V_g and source-drain bias V_{sd}, measured at $B_z = 4$ T. (c) Energy dependence dV_{sd}/dV_g plotted vs V_g, extracted at different fields B_z. The dashed line is a linear interpolation between values.

Fig. 3(c) to convert the gate voltage splitting δV_g at any B_z into a Zeeman splitting ΔE_Z according to Eqn 1.

The Zeeman energy obtained from the above measurements is plotted as a function of B_z for the three lowest subbands in Fig. 4. Reassuringly ΔE_Z grows linearly with B_z. We can also rule out the possibility that we are simply measuring the Landau level separation in the quantum Hall regime: This would give an apparent spin-splitting of $\hbar\omega_c/2$ independent of subband index, which is much larger than the slope of the lines we obtain.

The above extraction of the Zeeman splitting using using Eqn 1 explicitly assumes that the electrostatic potential in the wire is not affected by the magnetic field, which is not the case for B_z. Therefore we have measured the Zeeman splitting for $n = 3$ using a second, completely separate technique, based upon magnetic depopulation of hybrid magneto-electric subbands. Magnetic depopulation has previously been used to determine the eigenergies of spin degenerate 1D subbands[19,23,24], and the large InGaAs g-factor allows us to extend this technique to also measure the 1D Zeeman energy.

In the Landau gauge, the hybrid magneto-electric confinement in the QPC can be modeled as:

$$U^{\pm}_{hyb}(y) = U_0(y) + \frac{1}{2}m^*\omega_c^2 y^2 \pm \frac{|g_n^*|\mu_B B_z}{2} \qquad (2)$$

where $\omega_c = eB_z/m^*$ is the cyclotron frequency, $m^* = 0.038m_e$, and $\pm$ denotes up and down spins. The electrostatic confinement $U_0(y)$ is modeled as a flat-bottomed parabola of width t and curvature $\hbar\omega_0$.[19,24], and g_n is the g-factor of the n^{th} 1D subband. For a given Fermi energy (determined by V_g) the magnetic field at which the 1D subbands depopulate can be calculated from Eqn 2. This can then be compared with the measured magnetic fields at which the 1D subbands depopulate for a fixed V_g, indicated by the bright lines in Fig. 3(a), to extract U_0, t, $\hbar\omega_0$ and g_n.[19,24] It is only possible to obtain a well constrained set of fitting parameters if at least 3 of the 1D subbands depopulate at the same V_g, so it was only possible to extract the g-factor of the $n = 3$ subband with this technique. One complication of this technique is that it assumes that the field is low enough that the Fermi energy in the 2D reservoirs is approximately constant. However in the experiments the filling factor in the 2D reservoirs changes from $\nu = 10$ to $\nu = 4$ between $B_z = 3$ and 5 T, which can produce an oscillation of the Fermi level that is not accounted for in the depopulation method.

The Zeeman splittings extracted for $n = 3$ from the source-drain biasing and magnetic depopulation methods are plotted in Fig. 4 as solid and open triangles respectively. The data show a linear growth of E_z and good agreement between the two methods. This suggests that reliable g-factors can be extracted even in a perpendicular magnetic field, and these are plotted in Fig. 2(b). The g-factors for the B_z orientation are significantly larger than for in-plane fields, with a value of $|g_1^*| = 15.7$ for the 1st subband.

It is instructive to compare the 1D g-factors measured here with previous measurements in 2D $Ga_xIn_{1-x}As$ quantum wells. Kowalski *et al.* used optically detected magnetic resonance (ODMR) to probe the bare electron g-factor g as a function of gallium fraction x and field orientation.[4] Note that the ODMR measurements of the bare electron g-factor are very different to the g^* that we measure in our experiments, since ODMR is not affected by the exchange and correlation effects that enhance g^* in the quantum Hall regime. In Ref 4 it was found that the bare g-factor was maximum with the magnetic field oriented perpendicular to the quantum well, whereas a lower and isotropic g-factor was obtained for in-plane fields. The heterostructures used by Kowalski *et al.* were grown under similar conditions and contained quantum wells of similar width to ours, so we extrapolate their data to gallium fraction $x = 0.25$ (*c.f.* Fig. 2 of Ref. 4) to obtain 2D g-factors $|g| \approx 3.1$ for in-plane and $|g| \approx 5.2$ for perpendicular fields. We indicate these bare 2D g-factors with the arrows on the right hand side of Fig. 2(b). For in-plane fields and large 1D subband index, the g^* we

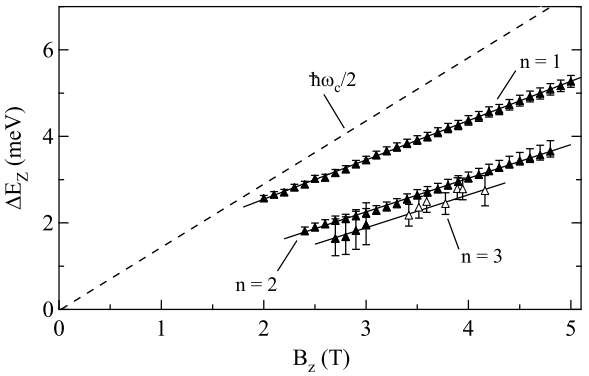

FIG. 4: Zeeman splitting ΔE_Z plotted vs magnetic field B_z applied perpendicular to the quantum well. For the $n = 3$ subband, solid triangles are obtained from the source-drain biasing method, and open triangles are obtained from the magnetic depopulation method. Solid lines show linear fits to the data.

measure tend towards the bare 2D limit. For lower 1D subband index the 1D confinement becomes stronger, exchange effects become more pronounced, and $|g^*|$ rises, reaching a maximum of approximately double the 2D result ($|g_1^*| = 6.2$ for B_y). The magnitude of the relative enhancement for $n = 1$ and the isotropy with respect to B_x and B_y match previous measurements in n-type GaAs QPCs.[7,8] In contrast, for perpendicular fields, our measured g^* are significantly larger than the ODMR bare g measurements, and do not approach the bare g-factor at large subband index, since ODMR is not sensistive to the strong oscillatory exchange enhancement that occurs in a perpendicular magnetic field.[13]

In summary, we have demonstrated a significant enhancement of the Zeeman spin-splitting in an InGaAs QPC for three orthogonal magnetic field directions. The largest value of $|g_1^*| = 15.7$ occurs in perpendicular fields for the lowest 1D subband. In agreement with theoretical predictions based on the exchange interaction,[13–15] all three field orientations show the largest enhancement for the $n = 1$ subband. Although the larger enhancement observed in perpendicular fields indicates that the additional orbital confinement strengthens the exchange enhancement, the magnitude of the enhancement is still much less than that predicted for infinite wires.[14,15] Models of infinite 1D wires for both in-plane[14] and perpendicular[15] orientations indicate that spin-polarization in the wires causes an exchange-enhanced Zeeman splitting. The 1D models also show an increase in enhancement as the subband occupation is reduced and the confinement strengthens.[14,15] This is in agreement with the results in Fig. 2(b) and previous experimental observations.[7–12] Wang and Berggren have pointed out that the assumption of an infinite wire may not be realistic for a short QPC coupled to 2D reservoirs, and that the 2D coupling will reduce the measured values of g^*.[14] For example, the magnitude of the exchange-enhancement observed in experiments is typically no more than a factor of two for electrons,[7,8,11] while the theory predicts an enhancement of order 10 or more.[14,15] More realistic calculations that include the 2D reservoirs, and the effect of B_z on the 2D Fermi energy, such as those carried out recently for $B = 0$,[26] could help to clarify the role of exchange enhancement in ballistic QPCs.

We acknowledge financial support from the Australian Research Council through the Discovery Projects Scheme, the National Science Foundation, the Research Corporation, the Swedish Foundation for Strategic Research, and the Swedish Research Council. A.R.H. acknowledges an ARC APF grant.

* Electronic address: Alex.Hamilton@unsw.edu.au

1 S. A. Wolf, D. D. Awschalom, R. A. Buhrman, J. M. Daughton, S. von Molnar, M. L. Roukes, A. Y. Chtchelkanova, and D. M. Treger, Science **294**, 1488 (2001).

2 D. L. Vehse, S. G. Hummel, H. M. Cox, F. DeRosa, and S. J. Allen, Phys. Rev. B **33**, 5862 (1986).

3 M. Dobers, J. P. Vieren, Y. Guldner, P. Bove, F. Omnes, and M. Razeghi, Phys. Rev. B **40**, 8075 (1989).

4 B. Kowalski, P. Omling, B. K. Meyer, D. M. Hofmann, C. Wetzel, V. Härle, F. Scholz, and P. Sobkowicz, Phys. Rev. B **49**, 14786 (1994).

5 T. Schäpers, V. A. Guzenko, and H. Hardtdegen, Appl. Phys. Lett. **90**, 122107 (2007).

6 J. Sun, M. Larsson, I. Maximov, H. Hardtdegen, and H. Q. Xu, Appl. Phys. Lett. **94**, 042114 (2009).

7 N. K. Patel, J. T. Nicholls, L. Martín-Moreno, M. Pepper, J. E. F. Frost, D. A. Ritchie, and G. A. C. Jones, Phys. Rev. B **44**, 10973 (1991).

8 K. J. Thomas, J. T. Nicholls, M. Y. Simmons, M. Pepper, D. R. Mace, and D. A. Ritchie, Phys. Rev. Lett. **77**, 135 (1996).

9 A. J. Daneshvar, C. J. B. Ford, A. R. Hamilton, M. Y. Simmons, M. Pepper, and D. A. Ritchie, Phys. Rev. B **55**, R13409 (1997).

10 R. Danneau, O. Klochan, W. R. Clarke, L. H. Ho, A. P. Micolich, M. Y. Simmons, A. R. Hamilton, M. Pepper, D. A. Ritchie, and U. Zülicke, Phys. Rev. Lett. **97**, 026403 (2006).

11 T. P. Martin, A. Szorkovszky, A. P. Micolich, A. R. Hamilton, C. A. Marlow, H. Linke, R. P. Taylor, and L. Samuelson, Appl. Phys. Lett. **93**, 012105 (2008).

12 T.-M. Chen, A. C. Graham, M. Pepper, F. Sfigakis, I. Farrer, and D. A. Ritchie, Phys. Rev. B **79**, 081301(R) (2009).

13 T. Ando and Y. Uemura, J. Phys. Soc. Jpn. **37**, 1044 (1974).

14 C.-K. Wang and K.-F. Berggren, Phys. Rev. B **54**, R14257 (1996).

15 S. Ihnatsenka and I. V. Zozoulenko, J. Phys.: Condens.

Matter **20**, 335233 (2008).
[16] D. Csontos and U. Zülicke, Appl. Phys. Lett. **92**, 023108 (2008).
[17] O. Klochan, A. P. Micolich, L. H. Ho, A. R. Hamilton, K. Muraki, and Y. Hirayama, New J. Phys. **11**, 043018 (2009).
[18] P. Ramvall, N. Carlsson, I. Maximov, P. Omling, L. Samuelson, W. Seifert, Q. Wang, and S. Lourdudoss, Appl. Phys. Lett. **71**, 918 (1997).
[19] T. P. Martin, C. A. Marlow, L. Samuelson, A. R. Hamilton, H. Linke, and R. P. Taylor, Phys. Rev. B **77**, 103811 (2008).
[20] B. J. van Wees, H. van Houten, C. W. J. Beenakker, J. G. Williamson, L. P. Kouwenhoven, D. van der Marel, and C. T. Foxon, Phys. Rev. Lett. **60**, 848 (1988).
[21] L. I. Glazman and A. V. Khaetskii, Europhys. Lett. **9**, 263 (1989).
[22] H. Xu, Phys. Rev. B **47**, 15630 (1993).
[23] K.-F. Berggren, T. J. Thornton, D. J. Newson, and M. Pepper, Phys. Rev. Lett. **57**, 1769 (1986).
[24] D. A. Wharam, U. Ekenberg, M. Pepper, D. G. Hasko, H. Ahmed, J. E. F. Frost, D. A. Ritchie, D. C. Peacock, and G. A. C. Jones, Phys. Rev. B **39**, 6283 (1989).
[25] C. W. J. Beenakker, H. van Houten, and B. J. van Wees, Superlatt. Microstruct. **5**, 127 (1989).
[26] P. Jaksch, I. Yakimenko, and K.-F. Berggren, Phys. Rev. B **74**, 235320 (2006).